Tracking of photospheric shock waves in computational fluid dynamics data

P. Leitner[1], T. Zaqarashvili[1,2,3], A. Hanslmeier[1], M. Temmer[1], A. Veronig[1], B. Lemmerer[1], H. Grimm-Strele[4,5], H.J. Muthsam[4]

[1] Institute of Physics - IGAM, University of Graz
[2] Space Research Institute, Austrian Academy of Sciences
[3] Abastumani Astrophysical Observatory at Ilia State University
[4] Faculty of Mathematics, University of Vienna
[5] Max-Planck Institute for Astrophysics, Garching

Outline

- **Present the ANTARES code/specific model photosphere**
- **Studies of our workgroup based on the obtained model data**
- **Describe shock wave detection algorithms**
- **Show first results obtained by post-processing application to our simulation data**

The ANTARES RHD code

- **Over more than a decade fully matured RHD code [Muthsam et al. 2007, 2010]**
- **Heavily under development with an imminent RMHD upgrade to be released**
- **Applications: photospheric turbulence [Muthsam et al. 2007], Cepheid pulsations [Muthsam et al. 2011], ...**

Recent developments:

- **Consideration of two-component flows [Zaussinger 2010]**
- **A parallel multigrid solver [Happenhofer et al. 2013]**
- **Solver for Navier-Stokes-Eqns on curvilinear grids [Grimm-Strele et al. 2014]**

Basic equations of radiation hydrodynamics

Continuity equation

$$\frac{\partial \varrho}{\partial t} + \nabla \cdot (\varrho \boldsymbol{u}) = 0$$

Euler's equation of momentum balance

$$\frac{\partial \varrho \boldsymbol{u}}{\partial t} + \nabla \cdot (\boldsymbol{M} - \sigma) = \boldsymbol{f}$$

Energy balance equation

$$\frac{\partial e}{\partial t} + \nabla \cdot \Big(\boldsymbol{u}(e + P) - \boldsymbol{u} \cdot \boldsymbol{\tau}\Big) = \varrho(\boldsymbol{g} \cdot \boldsymbol{u}) + Q_{\mathrm{rad}}$$

Radiation transfer equation

$$\hat{\boldsymbol{r}} \cdot \nabla I_\nu = \varrho \kappa_\nu (S_\nu - I_\nu)$$

The ANTARES code – Numerical schemes

- **ANTARES distinguished by its elaborate numerical schemes and numerical stability**
- **Finite volume methods are prone to numerical oscillations at discontinuities**
  - Traditional remedies:
    - Introduction of artificial viscosity
    - Application of limiters
  - In ANTARES weighted essentially non-oscillatory finite volume (WENO) schemes are implemented [Kupka et al. 2012]
- **Treatment of turbulence by adopting local mesh refinement**
- **Boundary conditions**
  - periodic for all quantities in horizontal directoins
  - open at the bottom and top: allowing for convective mass- and energy in- and outflow
  - transmissive for waves

Study of the photospheric structure

- **Studied vertical photospheric stratification and layers of distinguished dynamical characteristics by correlation analysis**

Astrophys Space Sci (2017) 362:181
DOI 10.1007/s10509-017-3151-7

CrossMark

ORIGINAL ARTICLE

Structure of the solar photosphere studied from the radiation hydrodynamics code ANTARES

P. Leitner[1] · B. Lemmerer[1] · A. Hanslmeier[1] · T. Zaqarashvili[1,2,3] · A. Veronig[1] ·
H. Grimm-Strele[4,5] · H.J. Muthsam[4]

Study of dynamical processes in the photosphere

Recently discovered small scale convective phenomena:

- **Small granules**
- **Intergranular plasma jets**

Pressure waves:

- **p-mode spectrum**
- **Shock waves (morphology, kinematics, energy transport)**

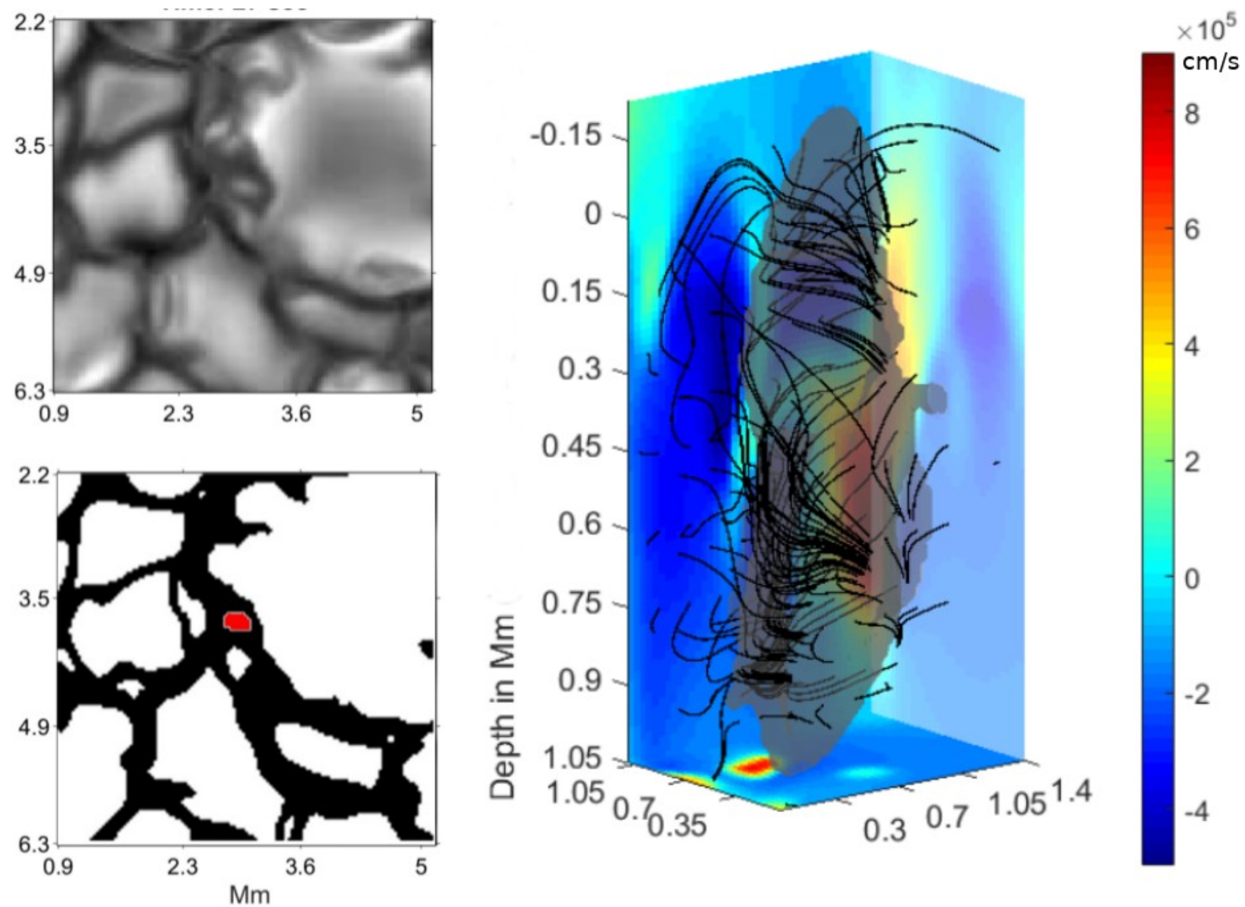

Left: Small granules, *Right:* Rotating plasma jets [Lemmerer et al. 2016]

Shock formation in the solar granulation

- **Overturning matter cools non-adiabatically turning transonic in highly localized regions**
- **Transition of transonic horizontal flows to turbulent subsonic downflows drives shock waves**
- **Shocks propagate upstream, weaken and finally dissolve**
- **Fluctuations are amplified by propagating shock waves**

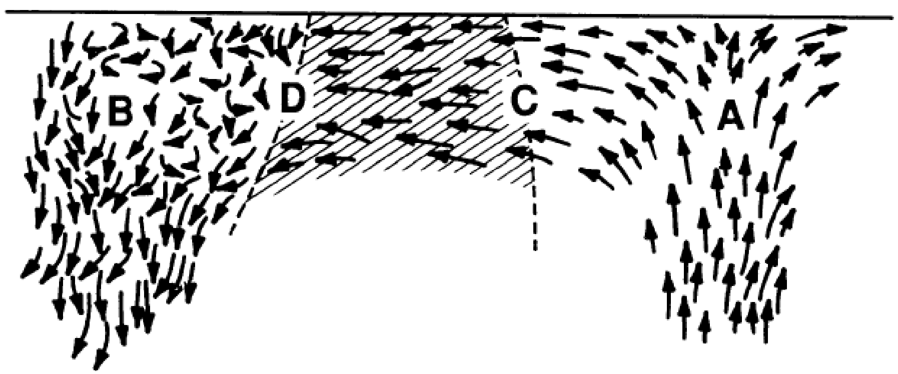

Supersonic horizontal flows at granular borders decelerat to subsonic velocities at (D). The abrupt transition corresponds to a shock wave.
From: A. Nesis, T.J. Bogdan, F. Cattaneo et al. 1992

Motivation for shock front segmentation

- **Mach number contours/isosurfaces also include oblique shocks**
- **Normal shock waves are subset of broader class of oblique shock waves**
- **→ Identification of surfaces where $M_\perp = 1$**
- **Workaround: Approximation of the direction normal by $\nabla\varrho$ [Ma et al. 1996], i.e.**

$$M_\perp \approx \frac{\boldsymbol{u}}{c_\mathrm{s}} \cdot \frac{\nabla\varrho}{\|\nabla\varrho\|}$$

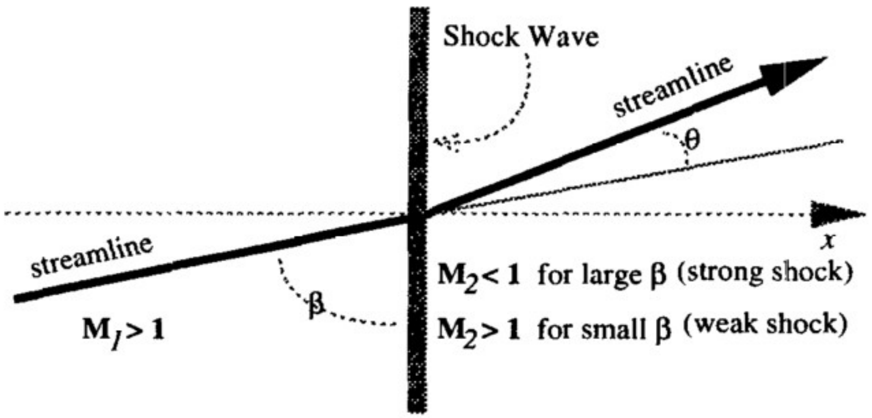

A 1-D oblique shock [Ma et al. 1996]

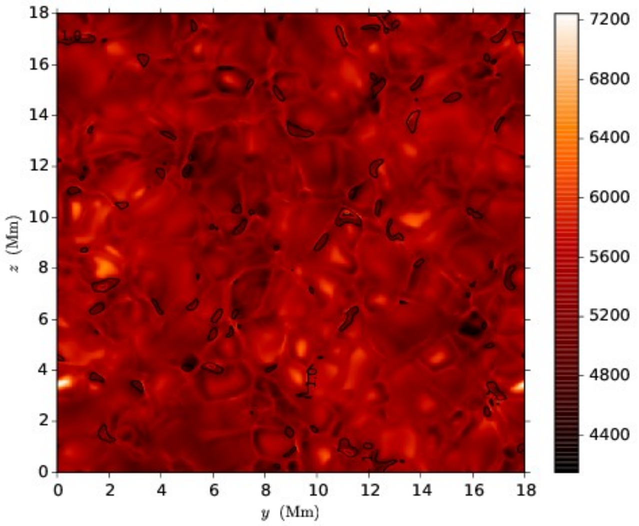

Post-processing techniques for shock detection:
1) Directional derivative thresholding [Pagendarm, H.G. and Seitz, B. 1993]

- **Location of a discontinuity can be approximated by the position of steepest gradient**

$$\delta_1 \varrho = \frac{\partial \varrho}{\partial n} = \frac{\boldsymbol{u}}{\|\boldsymbol{u}\|} \cdot \nabla \varrho \overset{!}{=} \max$$

$$\delta_2 \varrho = \frac{\partial^2 \varrho}{\partial n^2} = \frac{\boldsymbol{u}}{\|\boldsymbol{u}\|} \cdot \nabla \left(\frac{\boldsymbol{u}}{\|\boldsymbol{u}\|} \cdot \nabla \varrho \right) = 0$$

Shock detection procedure:

1) Evaluate first and second directional derivatives for all grid points

2) Construct zero-level iso-surfaces of the 2nd directional derivative

3) Discard points on these isosurfaces, where $\delta_1 \varrho < \epsilon$

4) Further discard points where $M_\perp \not\approx 1$

Application of procedure 1 to the ANTARES model atmosphere

- **Maxima of the directional density gradient (step 2, purple surfaces) fill large areas of the box**
- **Choose threshold value (step 3) as lower limit for first derivative (yellow surfaces)**
- **1-Isosurfaces of perp. Machnumber (step 4, green surfaces)**
- **Apply both filter on** $\delta_2 \varrho = 0$ **isosurfaces**

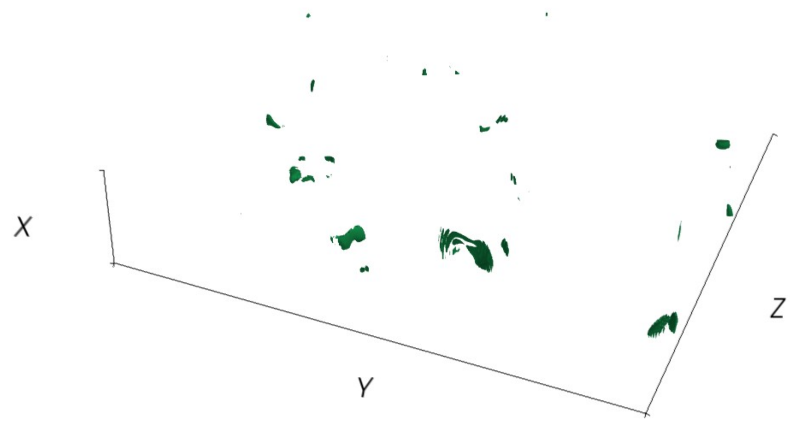

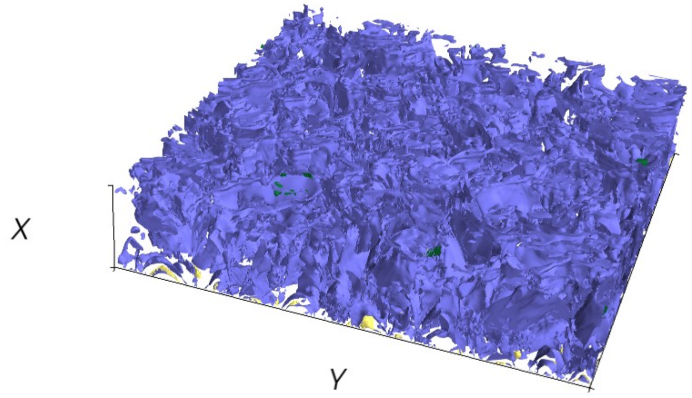

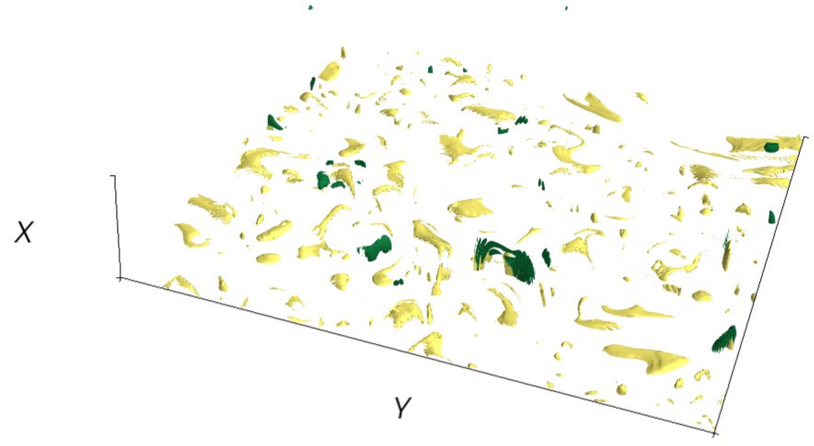

Shock wave detection procedure #2
Method based on normal Mach number by [Lovely and Hames 1999]

Method has 2 variants for detecting a) stationary and b) transient shocks

- **Variant a) is exactly filter number 4 of the preceding method**
- **Variant b) transient shocks; condition $M_{\perp}=1$ becomes**

$$\frac{1}{\|\nabla P\|}\cdot\frac{1}{c_{\mathrm{s}}}\cdot\frac{\mathrm{D}P}{\mathrm{D}t}=\frac{1}{\|\nabla P\|}\cdot\frac{1}{c_{\mathrm{s}}}\cdot\frac{\mathrm{d}P}{\mathrm{d}t}+\frac{\boldsymbol{M}\cdot\nabla P}{\|\nabla P\|}\overset{!}{=}1$$

- **Filters:**

$$\frac{|\nabla P\cdot\boldsymbol{n}|}{\|\nabla P\|}\leq c, \qquad \frac{\|\nabla P\|}{\|\nabla P\|_{\max}}\geq\eta$$

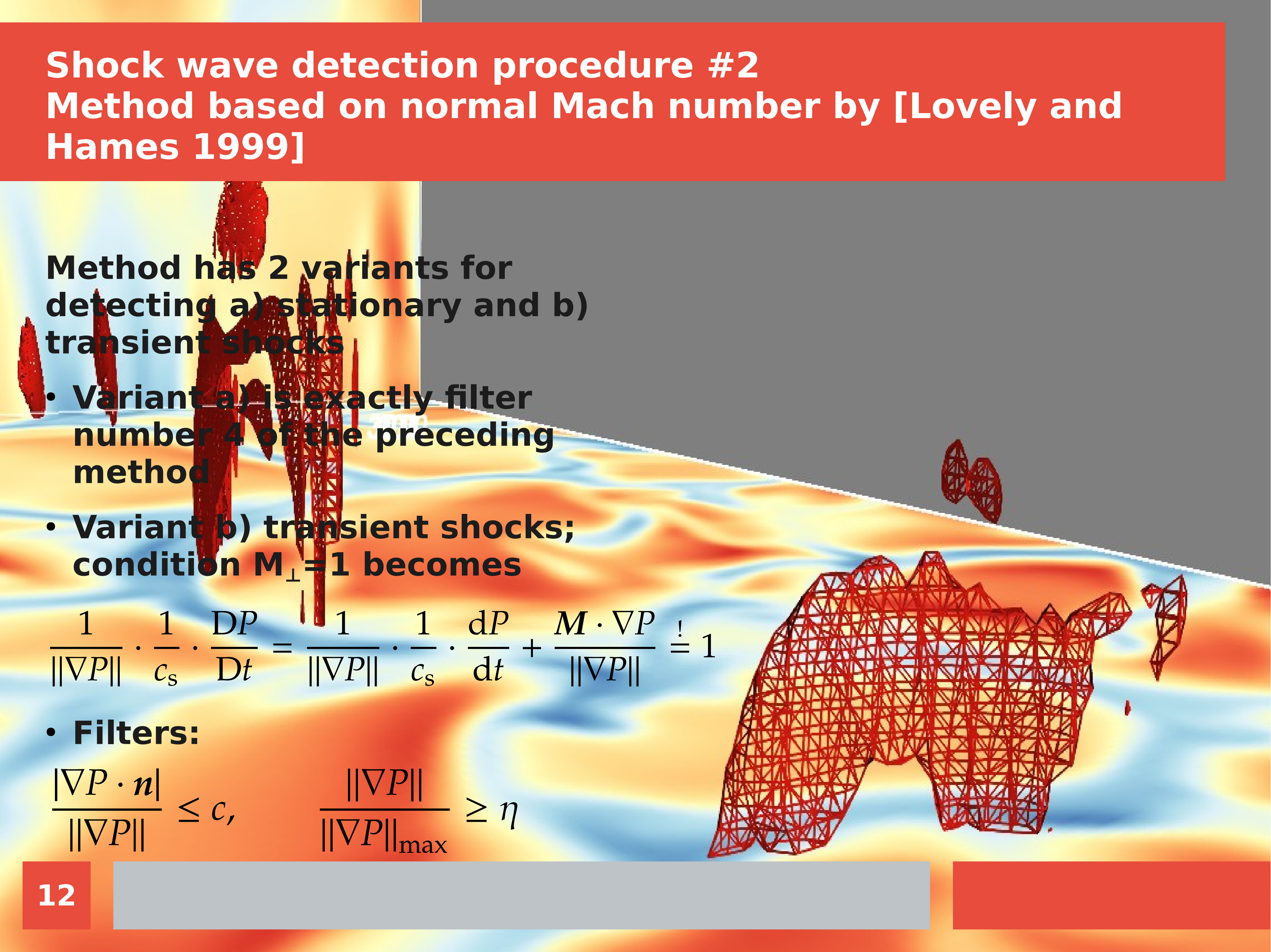

Results: Shock front segmentation for the ANTARES RHD model atmosphere

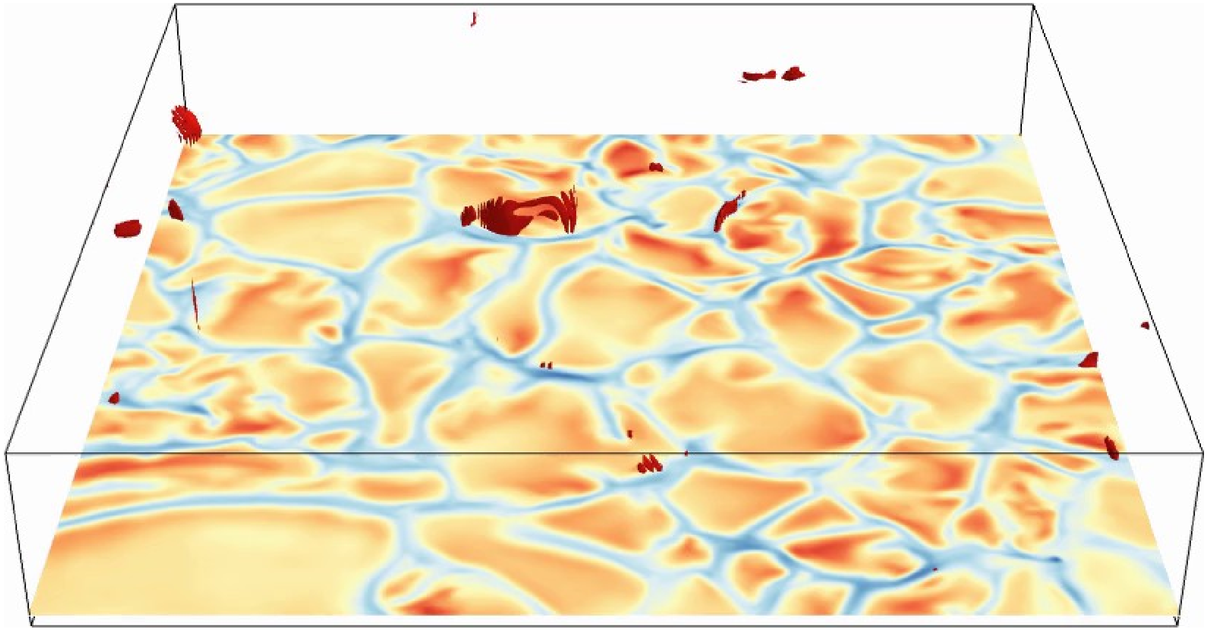

- Application of Lovely-Haimes algorithm for transient shock waves
- It needs to be further looked into how much the shock sizes are affected by fine-tuning paramters c and η

Comparison with shocks detected in RMHD data

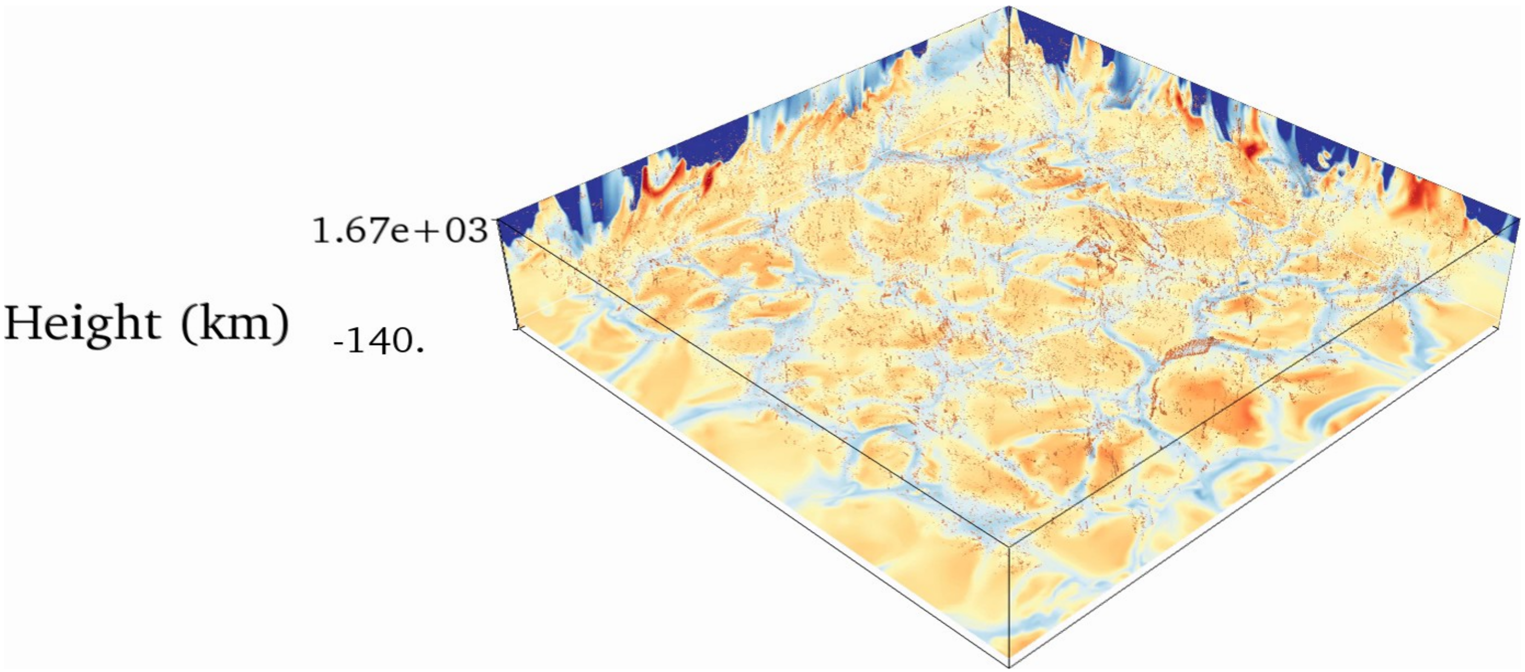

- **Application of Lovely-Haimes algorithm on CO5BOLD data**
- **Modified hydromagnetic energy jump-condition:**

$$\frac{1}{2}u_1^2 + \frac{\gamma}{\gamma-1}\frac{P_1}{\varrho_1} + \frac{B_1^2}{4\pi\varrho_1} = \frac{1}{2}u_2^2 + \frac{\gamma}{\gamma-1}\frac{P_2}{\varrho_2} + \frac{B_2^2}{4\pi\varrho_1}$$

Tracking of the temporal evolution of HD shock fronts

Study of shock propagation driven by aims:

- **Identification of the emission regions and wave drivers**
- **Study of the morphology and kinematics of photospheric shocks**
- **Quantification of the energy transport through shocked acoustic waves**
- **Location of height levels of wave dissipation within the photosphere**

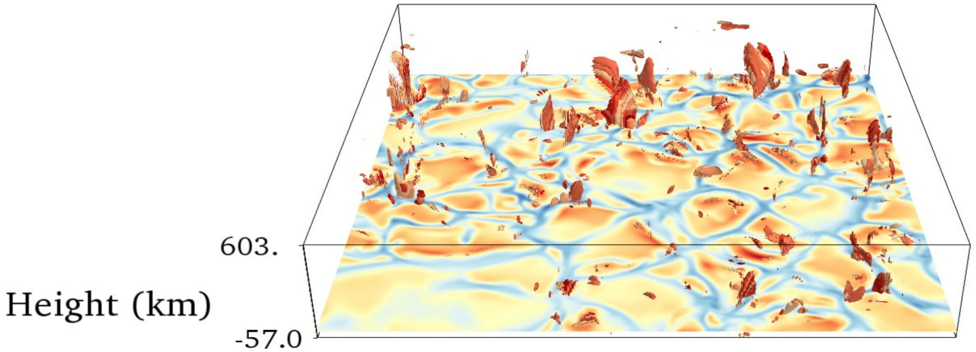

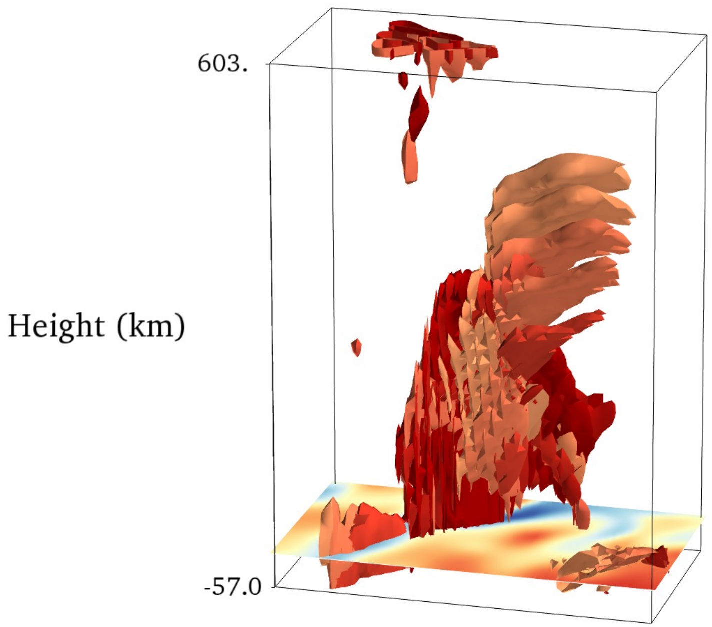

Case study:
i) Ascending shock

- **Using c.m. R_{cm} of segmented fronts for first rough description of the wave kinematics**
- **Emerges from below the photosphere**
- **Rises almost steadily to a height of $\approx$ 350 km before dissolution**
- **Propagation faster $\approx$ 5.5 km/s in ascending phase**
- **Horizontal velocity on average more than twice as large as vertical component**

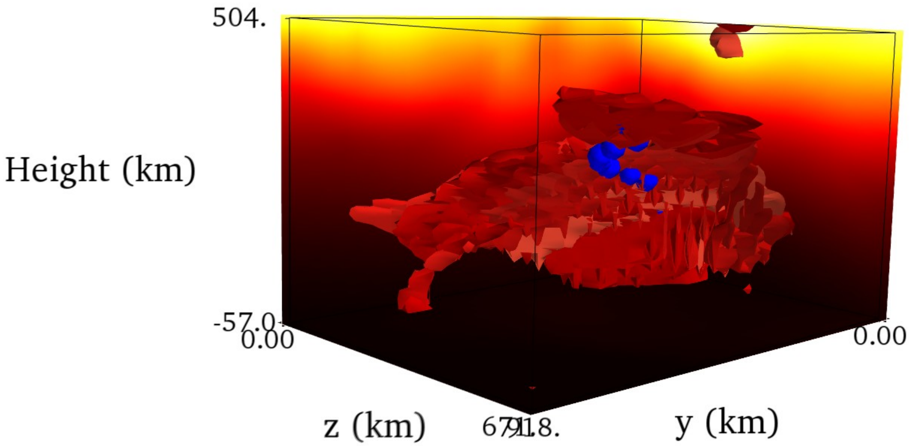

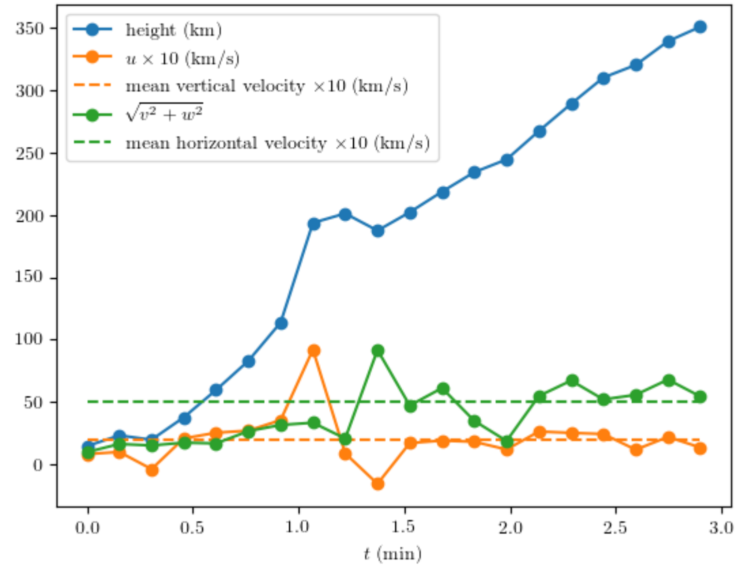

Case studies:
ii) Wave dissipation within the photosphere

- **Reaching point of highest ascent in the high photosphere then propagating downwards at ≈ 4 km/s, dissolving in the middle photosphere**
- **Descending waves at end of their lifetime slower than upwards moving waves emerging from the convection zone**
- **Vertical velocity component almost twice as large as the horizontal component**

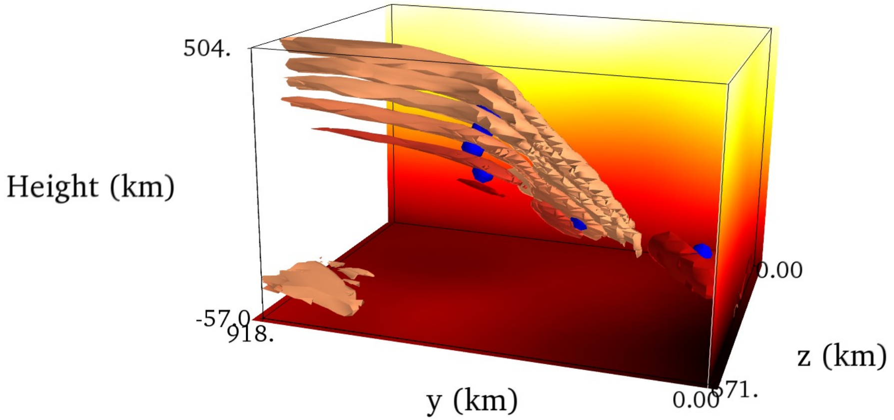

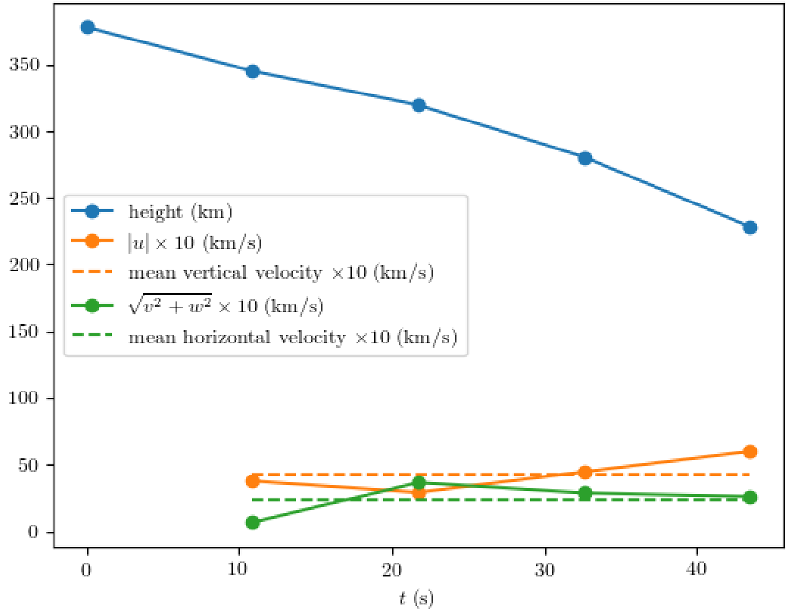

Case ii) Dissolution and dissipation of the descending shock wave

- **In all coordinate planes intersecting with $\boldsymbol{R_{\mathrm{cm}}(t_{\mathrm{fin}})}$ a small temperature increase in the vicinity is found**

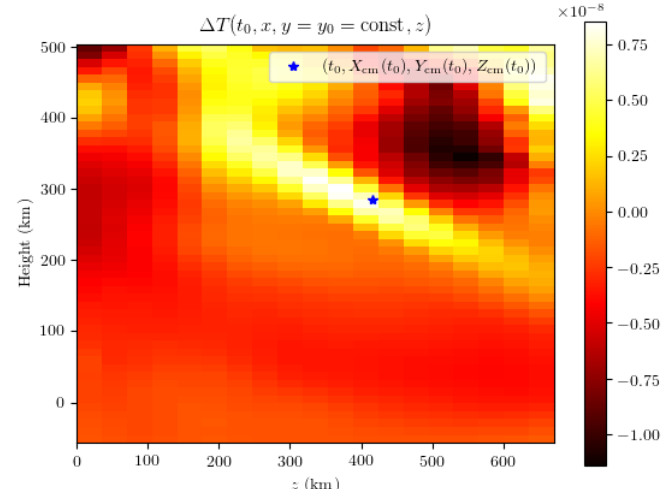

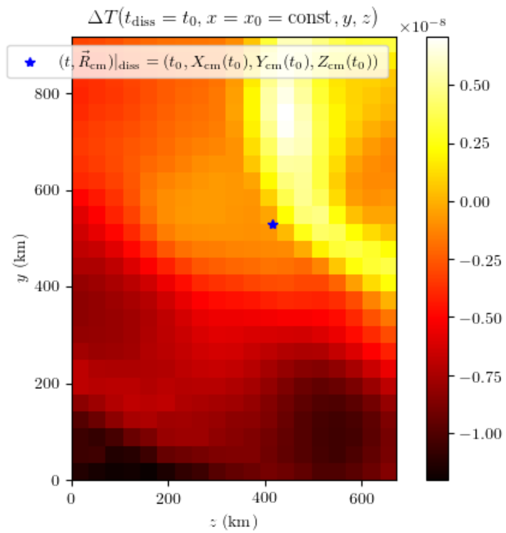

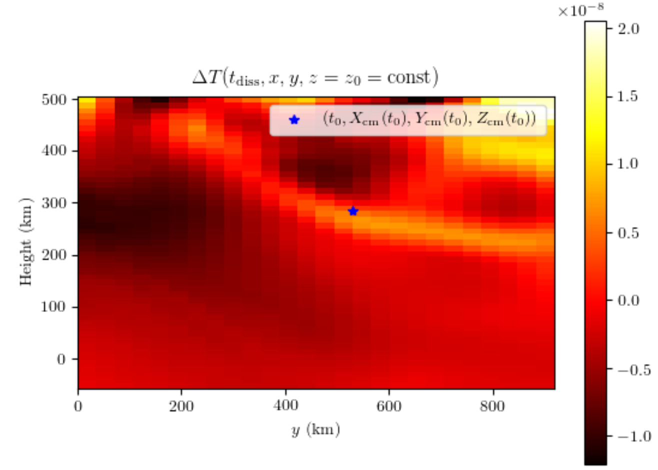

Correlation of shock fronts with the underlying flow pattern

- Propagation of shocks channelled in the intergranular lanes

- Correlation still very strong in the high photosphere

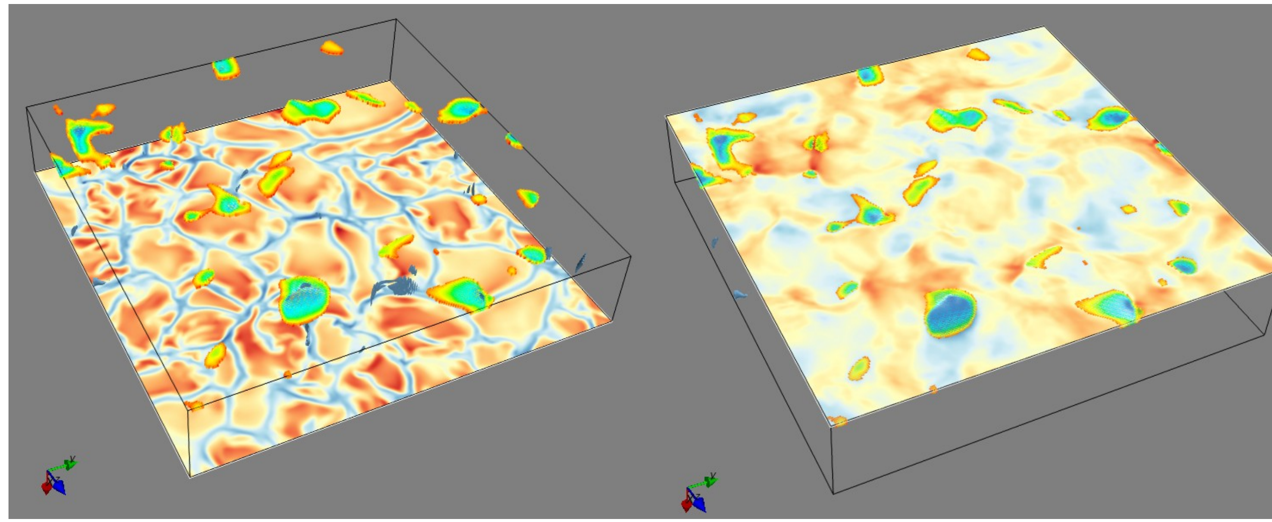

- Horizontal velocity increases with height, while vertical velocity is almost constant during ascending/descanding phases

- Maximum Machnumbers in the higher photosphere mostly in vertical flow component

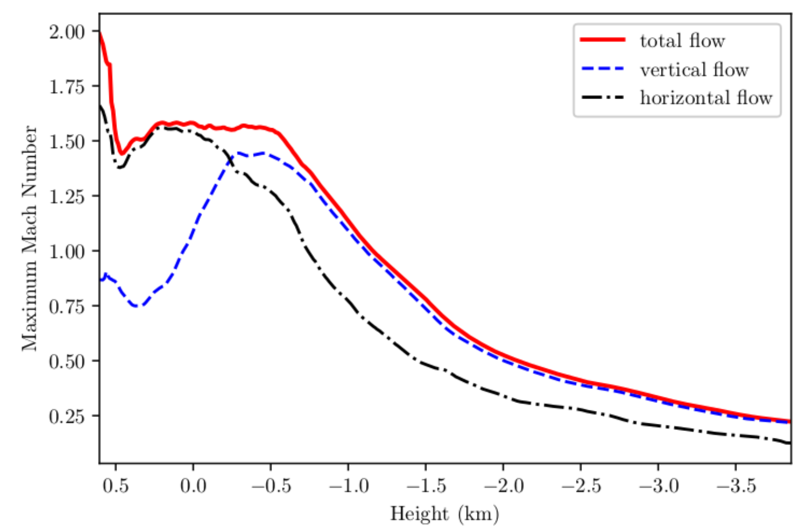

Outlook on further activities

- **Further case studies of wave propagation/statistical evaluation of shock wave kinematics**
- **ANTARES RMHD model photosphere**
  - Study Poynting flux and full hydromagnetic energy transport across the photosphere
  - Possibilty to study wave propagation into the chromosphere and quantify the heating of this layer due to acoustic and MHD waves
- **Comparison to observations**
  - Fine-tuning of threshold parameters from estimation of shock sizes

Summary

- **In parts, shocks emerge from below the photosphere inside the intergranular lanes**
- **High correlation between shock regions and intergranular flow field throughout the photosphere**
- **Some shocks turn over in the higher photosphere and descend again before dissolving and heating the surrounding matter**
- **Supersonic flows (possible drivers for shocks) found into a depth of 1.5 Mm below the surface**
- **In the higher photosphere it is mostly horizontal flows that are supersonic, below the surface also the vertical are found to turn transonic**